Inorganica Chimica Acta, *152* (1988) 25–36

Synthesis, Characterization and Antitumor Activity of some Metal Complexes of 3- and 5-Substituted Salicylaldehyde *o*-Hydroxybenzoylhydrazones

M. MOHAN*, N. S. GUPTA, M. P. GUPTA, A. KUMAR, M. KUMAR

Department of Chemistry, N.R.E.C. College, Khurja-203131, India

and N. K. JHA

Department of Chemistry, Indian Institute of Technology, Hauz Khas, New Delhi-110016, India

(Received October 7, 1987)

Abstract

Complexes of Mn(II), Fe(III), Fe(II), Co(II), Ni(II), Cu(II), Zn(II) and Pt(II) with 3- and 5-substituted salicylaldehyde *o*-hydroxybenzoylhydrazones (XSBH, X = H, $3\text{-}NO_2$, $3\text{-}CH_3O$, 5-Cl, 5-Br, $5\text{-}CH_3$ or $5\text{-}NO_2$) have been prepared and characterized by elemental analysis, conductance measurements, magnetic susceptibilities (from room temperature down to liquid nitrogen temperature) and spectral studies. These studies indicate the following structures: monomeric, high-spin, distorted octahedral for $Mn(XSBH)_2$; monomeric, high-spin, five-coordinate for $Fe(XSBH)SO_4\cdot H_2O$; dimeric, high-spin phenoxide bridged, five-coordinate for Fe(XSBH)Cl; dimeric, high-spin five-coordinate for $Co(XSBH)Cl\cdot 2H_2O$; dimeric low-spin, five-coordinate for $Ni(XSBH)Cl\cdot 2H_2O$; dimeric, four-coordinate for Zn(XSBH); and a square-planar structure for $M(XSBH)Cl\cdot H_2O$ (M = Cu(II) or Pt(II).

Intermolecular antiferromagnetic exchange interactions are present in Fe(III) complexes, where the exchange parameter (J) is *ca.* $-8.0\ cm^{-1}$ for these complexes. The Fe(III) complexes exhibit asymmetric quadrupole split doublets in their ^{57}Fe Mössbauer spectra. The asymmetry is found to be temperature dependent with relatively symmetrical doublets seen at low temperature. The polycrystalline ESR spectra of Cu(II) complexes are isotropic and indicate a $d_{x^2-y^2}$ ground state in square-planar stereochemistry. All these metal complexes have been screened for their antitumor activity against the P388 lymphocytic leukaemia test system in mice and enhanced antitumor activity relative to the free ligand was found but no significant activity at the dosages used.

Introduction

Aroylhydrazones of *o*-hydroxyaldehyde and ketones possess a third potent coordination site which makes them tridentate ligands [1]. These compounds have modest bacteriostatic properties when tested *in vitro* against microorganisms. Recently, aroylhydrazones, *i.e.* salicylaldehyde benzoylhydrazone, have been shown to be able to induce iron excretion in mammals and thus are potentially of use in the treatment of iron overload in man [2, 3]. This hydrazone is an unusually potent inhibitor of DNA synthesis in a variety of cultured human and rodent cells and its copper complex produces significant inhibition of tumor growth in mice [4].

In continuation of our previous work [5, 6], we report here the preparation of metal(II) and metal(III) complexes with 3- and 5-substituted salicylaldehyde *o*-hydroxybenzoylhydrazones (XSBH) and their antitumor activity against the P388 lymphocytic leukaemia test system in mice.

Experimental

Materials

Salicylaldehyde, 3-methoxysalicylaldehyde (*o*-vanillin), and *o*-hydroxybenzoylhydrazide were obtained from Aldrich Chemical Co., U.S.A., and used without further purification. 5-Chlorosalicylaldehyde and 3- and 5-nitrosalicylaldehyde were obtained from Eastman Chemical Co., U.S.A. All other chemicals and solvents were of Reagent grade or equivalent.

5-Bromosalicylaldehyde was prepared by adding bromine to an equivalent amount of a cold solution of salicylaldehyde dissolved in glacial acetic acid. 5-Methylsalicylaldehyde was prepared by a modification of the Reimer–Tieman reaction, using *p*-cresol and chloroform in a highly alkaline medium.

3- and 5-Substituted salicylaldehyde *o*-hydroxybenzoylhydrazones were prepared according to the reported procedure [5]. The authenticity of the compounds was checked by melting points, IR and TLC.

Synthesis

All the metal complexes were obtained by the following general method. A hot solution of the

---

*Author to whom correspondence should be addressed.

0020-1693/88/$3.50

TABLE I. Analytical Data of the Metal Complexes

Compound	Colour	Found (%)				Calculated (%)			
		C	H	N	M	C	H	N	M
H–SBH	white	65.64	4.70	10.95		65.62	4.68	10.94	
3-NO_2SBH	white	55.82	3.66	13.97		55.31	3.65	13.95	
3-CH_3O·SBH	white	62.95	4.90	9.81		62.93	4.89	9.79	
5-ClSBH	white	57.86	3.79	9.65		57.83	3.78	9.63	
5-BrSBH	white	50.18	3.30	8.37		50.16	3.28	8.36	
5-CH_3SBH	white	66.68	5.20	10.38		66.66	5.18	10.37	
5-NO_2SBH	white	55.83	3.66	13.97		55.81	3.65	13.95	
Mn(H-SBH)$_2$	light yellow	59.48	3.91	9.96	9.72	59.47	3.89	9.91	9.69
Mn(3-NO_2SBH)$_2$	yellow	51.01	3.05	8.51	8.36	50.99	3.03	8.49	8.33
Mn(3-CH_3OSBH)$_2$	yellow	55.69	3.70	8.98	8.80	55.68	3.68	8.96	8.78
Mn(5-ClSBH)$_2$	light yellow	52.94	3.15	8.83	8.67	52.91	3.14	8.81	8.65
Mn(5-BrSBH)$_2$	dark yellow	46.49	2.79	7.77	7.61	46.47	2.76	7.74	7.59
Mn(5-CH_3SBH)$_2$	yellow	58.52	3.87	9.43	9.26	58.49	3.86	9.41	9.23
Mn(5-NO_2SBH)$_2$	yellow	51.01	3.05	8.51	8.36	50.99	3.03	8.49	8.33
Fe(H–SBH)Cl	black	48.38	3.17	8.08	16.09	48.36	3.16	8.06	16.07
Fe(3-NO_2SBH)Cl	black	42.93	2.82	10.72	14.26	42.92	2.80	10.70	14.23
Fe(3-CH_3OSBH)Cl	dark green	47.59	3.72	7.72	14.77	47.57	3.70	7.70	14.74
Fe(5-ClSBH)Cl	green	43.90	2.88	9.34	14.60	43.88	2.87	9.33	14.58
Fe(5-BrSBH)Cl	black	39.33	2.59	6.56	13.07	39.31	2.57	6.55	13.06
Fe(5-CH_3SBH)Cl	green	49.69	3.87	7.74	15.44	49.67	3.86	7.72	15.41
Fe(5-NO_2SBH)Cl	dark green	42.94	2.82	10.73	14.25	42.92	2.80	10.70	14.23
Fe(H–SBH)SO_4·H_2O	dark brown	39.36	3.07	6.59	13.13	39.35	3.04	6.57	13.11
Fe(3-NO_2SBH)SO_4·H_2O	brown	35.63	2.77	8.92	11.85	35.60	2.75	8.90	11.83
Fe(3-CH_3OSBH)SO_4·H_2O	brown	39.43	3.54	6.54	12.24	39.40	3.50	6.52	12.22
Fe(5-ClSBH)SO_4·H_2O	light brown	36.42	2.83	6.08	12.11	36.41	2.81	6.06	12.10
Fe(5-BrSBH)SO_4·H_2O	reddish brown	33.24	2.58	5.60	11.05	33.21	2.56	5.58	11.03
Fe(5-CH_3SBH)SO_4·H_2O	dark brown	40.85	3.65	6.37	12.68	40.83	3.62	6.35	12.66
Fe(5-NO_2SBH)SO_4·H_2O	brown	35.63	2.78	8.92	11.86	35.60	2.75	8.90	11.83
Co(H–SBH)Cl·2H_2O	brown	43.41	3.90	7.25	15.27	43.40	3.88	7.24	15.24
Co(3-NO_2SBH)Cl·2H_2O	dark brown	38.86	3.48	9.74	13.64	38.85	3.46	9.71	13.62
Co(3-CH_3OSBH)Cl·2H_2O	brown	43.14	4.32	6.72	14.13	43.12	4.31	6.70	14.11
Co(5-ClSBH)Cl·2H_2O	brown	39.84	3.57	6.64	13.98	39.81	3.55	6.63	13.96
Co(5-BrSBH)Cl·2H_2O	dark brown	36.03	3.24	6.04	12.65	36.01	3.21	6.00	12.63
Co(5-CH_3SBH)Cl·2H_2O	brown	44.86	4.49	6.99	14.70	44.83	4.48	6.97	14.68
Co(5-NO_2SBH)Cl·2H_2O	brown	38.87	3.49	9.72	13.64	38.85	3.46	9.71	13.62
Ni(H–SBH)Cl·2H_2O	green	43.52	3.91	7.26	15.22	43.49	3.88	7.24	15.20
Ni(3-NO_2SBH)Cl·2H_2O	green	38.97	3.26	9.76	13.64	38.96	3.24	9.74	13.61
Ni(3-CH_3OSBH)Cl·2H_2O	yellowish green	43.27	4.09	6.74	14.92	43.24	4.08	6.72	14.90
Ni(5-ClSBH)Cl·2H_2O	green	39.95	3.35	6.67	13.96	39.93	3.32	6.65	13.95
Ni(5-BrSBH)Cl·2H_2O	green	36.26	3.02	6.06	12.62	36.23	3.00	6.03	12.59
Ni(5-CH_3SBH)Cl·2H_2O	green	44.88	4.26	6.98	14.65	44.86	4.23	6.97	14.63
Ni(5-NO_2SBH)Cl·2H_2O	green	38.98	3.27	9.76	13.62	38.96	3.24	9.74	13.61
Cu(H–SBH)Cl·H_2O	dark green	45.04	4.02	7.52	17.09	45.01	4.01	7.50	17.07
Cu(3-NO_2SBH)Cl·H_2O	green	40.19	3.36	10.07	15.24	40.17	3.34	10.04	15.23
Cu(3-CH_3OSBH)Cl·H_2O	black	44.67	4.23	6.97	15.92	44.64	4.21	6.94	15.90
Cu(5-ClSBH)Cl·H_2O	black	41.23	3.46	6.87	15.64	41.20	3.43	6.86	15.62
Cu(5-BrSBH)Cl·H_2O	dark green	37.09	3.09	6.19	14.07	37.06	3.08	6.17	14.05
Cu(5-CH_3SBH)Cl·H_2O	dark green	46.38	4.39	7.24	16.42	46.36	4.37	7.21	16.41
Cu(5-NO_2SBH)Cl·H_2O	green	40.19	3.35	10.06	15.25	40.17	3.34	10.04	15.23
Zn(H–SBH)	light yellow	52.28	3.45	8.72	20.36	52.27	3.42	8.71	20.34
Zn(3-NO_2SBH)	yellow	45.87	2.76	11.47	17.86	45.84	2.72	11.46	17.84
Zn(3-CH_3OSBH)	yellow	51.23	3.71	7.97	18.63	51.22	3.69	7.96	18.60
Zn(5-ClSBH)	light yellow	47.09	2.81	7.86	18.34	47.07	2.80	7.84	18.31
Zn(5-BrSBH)	dark yellow	41.86	2.52	6.98	16.30	41.85	2.49	6.96	16.28
Zn(5-CH_3SBH)	yellow	53.52	3.87	8.34	19.46	53.51	3.86	8.32	19.43
Zn(5-NO_2SBH)	light yellow	45.85	2.74	11.47	17.85	45.84	2.72	11.46	17.84

(continued)

TABLE I. *(continued)*

Compound	Colour	Found (%)				Calculated (%)			
		C	H	N	M	C	H	N	M
$Pt(H{-}SBH)Cl \cdot H_2O$	dark red	33.32	2.59	5.56	38.68	33.29	2.57	5.54	38.66
$Pt(3\text{-}NO_2SBH)Cl \cdot H_2O$	red	30.58	2.20	7.63	35.42	30.56	2.18	7.60	35.41
$Pt(3\text{-}CH_3OSBH)Cl \cdot H_2O$	red	33.69	2.31	5.25	36.52	33.68	2.80	5.23	36.49
$Pt(5\text{-}ClSBH)Cl \cdot H_2O$	black	31.19	2.25	5.20	36.20	31.16	2.22	5.19	36.18
$Pt(5\text{-}BrSBH)Cl \cdot H_2O$	black	28.75	2.06	4.79	33.32	28.73	2.04	4.78	33.30
$Pt(5\text{-}CH_3SBH)Cl \cdot H_2O$	red	34.66	2.90	5.39	37.52	34.64	2.88	5.38	37.50
$Pt(5\text{-}NO_2SBH)Cl \cdot H_2O$	dark red	30.58	2.20	7.61	35.42	30.56	2.18	7.60	35.41

ligand (1 mmol) in ethanol (25 ml) was added to a hot solution of the metal salt (1 mmol) in ethanol (25 ml) or an aqueous solution of K_2PtCl_4 (1 mmol), with constant stirring. The dark coloured solution mixture was refluxed for 2–3 h and allowed to stand at room temperature overnight when the crystalline complex was precipitated. The solid was filtered, washed successively with EtOH and Et_2O and then dried *in vacuo* over P_2O_5.

Physical Measurements

Physical measurements were carried out as described previously [5]. The analytical data of ligands and their metal complexes are summarized in Table I.

Results and Discussion

The infrared spectra of free XSBH ligands exhibit ν(N–H) absorption bands at *ca.* 3275 and *ca.* 3210 cm^{-1} and ν(C=O) at *ca.* 1670 cm^{-1}, suggesting that the ligands exist in the keto form **I** in the solid state. However, in solution and in the presence of metal ions, the ligands may exist in equilibrium with the tautomeric enol form **II**. Tautomer **II**, by loss of the enolic and phenolic protons, may act as a doubly charged tridentate ligand coordinating through the phenolic oxygen, the azomethine nitrogen and the carbonyl oxygen atoms. When the hot solution of the ligand is refluxed with an ethanolic or aqueous solution of the metal salt, shiny coloured crystalline solids of the formula $Mn(XSBH)_2$, Fe(XSBH)Cl, $Fe(XSBH)SO_4 \cdot H_2O$, $M(XSBH)Cl \cdot 2H_2O$ (M = Co(II) or Ni(II)), $M(XSBH)Cl \cdot H_2O$ (M = Cu(II) or Pt(II)) and Zn(XSBH) were obtained. All the complexes except those with Fe(III), Co(II), Ni(II) and Zn(II) are soluble in water and other organic solvents. The molar conductances of these complexes in ethanol at *ca.* 10^{-3} M at 27 °C are in the range 8.0–14.0 ohm^{-1} cm^2 mol^{-1}, indicating non-electrolytic behaviour in solution [7].

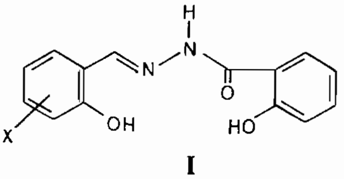

I

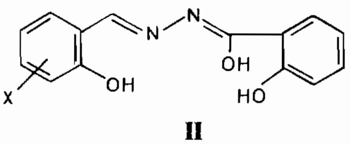

II

X = H, $3\text{-}NO_2$, $3\text{-}CH_3O$, 5-Cl, 5-Br, $5\text{-}CH_3$ or $5\text{-}NO_2$

The infrared spectra of free ligands exhibit bands at *ca.* 3440, *ca.* 3380 and *ca.* 2800 cm^{-1} which are assigned to ν_{as}(OH), ν_s(OH) and the intramolecularly hydrogen-bonded hydroxyl group of the phenolic group, respectively [8]. These absorption bands disappear in their metal complexes. The phenolic ν(C–O) stretching and bending vibrations observed at *ca.* 1520 and *ca.* 1280 cm^{-1}, respectively, in the free ligands XSBH are displaced to higher frequency by 25 cm^{-1} in the Fe(III), Co(II), Ni(II) and Zn(II) complexes, while in the Mn(II), Fe(II), Cu(II) and Pt(II) complexes these are not much disturbed. The upward shift of bands is a definite proof of the dimeric nature of the Fe(III), Co(II), Ni(II) and Zn(II) complexes involving phenoxide bridging [9, 10]. The shifting of the bands is probably due to the increase in C–O bond strength on extended delocalization of the π system of the azine moiety. This is further confirmed by the appearance of a

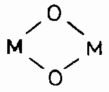

ring vibration at 725–735 cm^{-1} [11, 12].

In the NH stretching region, the high frequency component ν_{as}(NH) remains unchanged on coordination, relative to that of the free ligands, while the low frequency spectral band ν_s(NH) is shifted to higher frequency by *ca.* 50 cm^{-1} in the Mn(II), Fe(III), Fe(II), Cu(II) and Pt(II) complexes. This suggests that the ligands exist in the keto form in these complexes

TABLE II. Magnetic Susceptibility Data of the Metal Complexes

Mn(H–SBH)$_2$	T (K)	298.7	270.5	212.4	190.0	154.5	110.2	96.4	78.0
$\theta = -6.5$ K	χ_M (cgsu)	15077	16649	21132	23624	28955	40595	46251	57162
	μ_{eff} (μ_B)	6.00	6.00	5.99	5.99	5.88	5.98	5.97	5.97
Mn(3-NO$_2$SBH)$_2$	T (K)	300.0	278.5	216.0	209.0	166.3	108.7	97.4	78.0
$\theta = -5.0$ K	χ_M (cgsu)	15012	16170	20711	21404	26811	40880	45623	56780
	μ_{eff} (μ_B)	6.00	6.00	5.98	5.98	5.97	5.96	5.96	5.95
Mn(3-CH$_2$OSBH)$_2$	T (K)	297.8	276.0	216.7	207.4	167.3	109.6	96.8	78.0
$\theta = -6.6$ K	χ_M (cgsu)	15072	16263	20644	21570	26650	40680	45906	56971
	μ_{eff} (μ_B)	5.99	5.99	5.98	5.98	5.97	5.97	5.96	5.96
Mn(5-ClSBH)$_2$	T (K)	298.8	268.6	218.5	206.6	168.4	108.2	97.2	78.0
$\theta = -6.5$ K	χ_M (cgsu)	14971	16655	20474	21581	26476	410691	45717	56971
	μ_{eff} (μ_B)	5.98	5.98	5.98	5.97	5.97	5.96	5.96	5.96
Mn(5-BrSBH)$_2$	T (K)	296.9	274.2	212.6	208.4	165.2	107.7	96.2	78.0
$\theta = -6.5$ K	χ_M (cgsu)	15168	16424	21183	21538	27170	41537	46503	57354
	μ_{eff} (μ_B)	6.00	6.00	6.00	5.99	5.99	5.98	5.98	5.98
Mn(5-CH$_3$SBH)$_2$	T (K)	296.8	273.6	213.0	206.0	164.2	107.0	98.0	78.0
$\theta = -6.0$ K	χ_M (cgsu)	15173	16405	21073	21716	27153	41669	45344	56971
	μ_{eff} (μ_B)	6.00	5.99	5.99	5.98	5.97	5.97	5.96	5.96
Mn(5-NO$_2$SBH)$_2$	T (K)	298.2	270.4	212.5	207.8	162.4	106.6	97.8	78.0
$\theta = -6.4$ K	χ_M (cgsu)	15052	16599	21122	21528	27546	41826	45589	57162
	μ_{eff} (μ_B)	5.99	5.99	5.99	5.98	5.98	5.97	5.97	5.97
Fe(H–SBH)Cl	T (K)	297.2	272.6	219.5	206.8	163.6	107.8	97.2	78.0
$J = -8.0$ cm^{-1}	χ_M (cgsu)	11453	12165	13975	14652	16518	19403	19556	20082
	μ_{eff} (μ_B)	5.21	5.15	4.95	4.92	4.64	4.06	3.89	3.53
Fe(3-NO$_2$SBH)Cl	T (K)	300.0	268.0	219.0	206.8	162.0	106.0	96.0	78.0
$J = -7.8$ cm^{-1}	χ_M (cgsu)	11452	12424	14099	14806	16699	19432	19249	20352
	μ_{eff} (μ_B)	5.24	5.15	4.94	4.95	4.65	4.05	3.84	3.56
Fe(3-CH$_3$OSBH)Cl	T (K)	300.0	269.0	218.0	205.0	164.0	118.0	97.0	78.0
$J = -7.8$ cm^{-1}	χ_M (cgsu)	11452	12424	14099	14748	16712	19053	19417	20352
	μ_{eff} (μ_B)	5.24	5.17	4.95	4.91	4.68	4.24	3.88	3.56
Fe(5-ClSBH)Cl	T (K)	298.2	258.0	220.0	188.6	148.0	110.6	96.2	78.0
$J = -8.0$ cm^{-1}	χ_M (cgsu)	11452	12717	14099	15413	17283	19504	19764	20790
	μ_{eff} (μ_B)	5.22	5.12	4.98	4.82	4.52	4.15	3.91	3.60
Fe(5-BrSBH)Cl	T (K)	298.6	260.0	219.2	190.2	144.8	109.2	96.8	78.0
$J = 8.1$ cm^{-1}	χ_M (cgsu)	11228	12379	13896	15039	16687	17927	19730	19659
	μ_{eff} (μ_B)	5.17	5.07	4.93	4.73	4.39	4.31	3.90	3.50
Fe(5-CH$_3$SBH)Cl	T (K)	298.7	262.2	219.7	192.4	152.2	108.7	97.8	78.0
$J = -7.9$ cm^{-1}	χ_M (cgsu)	11391	12497	13681	153031	17150	19352	19634	20094
	μ_{eff} (μ_B)	5.21	5.19	4.90	4.85	4.56	4.10	3.56	3.54
Fe(5-NO$_2$SBH)Cl	T (K)	297.6	264.5	217.6	193.3	154.2	107.8	98.2	78.0
$J = -8.2$ cm^{-1}	χ_M (cgsu)	11375	12278	13896	15023	17571	17875	19249	19874
	μ_{eff} (μ_B)	5.20	5.09	4.91	4.81	4.65	3.92	3.88	3.52
Fe(H–SBH)SO$_4$·H$_2$O	T (K)	296.8	261.5	218.2	190.5	153.4	106.7	97.2	78.0
$\theta = -3.5$ K	χ_M (cgsu)	11750	13286	15502	17484	21545	30256	32952	41064
	μ_{eff} (μ_B)	5.28	5.27	5.20	5.16	5.14	5.08	5.06	5.06
Fe(3-NO$_2$SBH)SO$_4$·H$_2$O	T (K)	296.2	263.4	217.6	195.5	154.7	108.7	96.8	78.0
$\theta = -3.0$ K	χ_M (cgsu)	11774	13140	15545	17169	21281	29816	33351	41064
	μ_{eff} (μ_B)	5.28	5.26	5.20	5.18	5.13	5.09	5.08	5.06
Fe(3-CH$_3$OSBH)SO$_4$·H$_2$O	T (K)	300.0	264.0	218.0	195.7	152.0	109.0	96.0	78.0
$\theta = -4.0$ K	χ_M (cgsu)	11669	13110	15636	17086	21744	29851	33628	40902
	μ_{eff} (μ_B)	5.29	5.26	5.22	5.17	5.14	5.10	5.08	5.05

(continued)

TABLE II. *(continued)*

$\mathrm{Fe(5\text{-}ClSBH)SO_4\cdot H_2O}$	T (K)	300.0	266.4	219.0	194.0	154.0	107.0	96.2	78.0
$\theta = -4.0$ K	χ_M (cgsu)	11616	12883	15433	172880	22444	30504	33664	41193
	μ_{eff} (μ_B)	5.28	5.24	5.20	5.18	5.14	5.11	5.09	5.07
$\mathrm{Fe(5\text{-}BrSBH)SO_4\cdot H_2O}$	T (K)	299.0	264.4	221.0	192.0	153.0	106.7	94.8	78.0
$\theta = -3.0$ K	χ_M (cgsu)	11664	12892	15188	17348	21434	30375	33950	41064
	μ_{eff} (μ_B)	5.26	5.22	5.18	5.16	5.12	5.09	5.07	5.06
$\mathrm{Fe(5\text{-}CH_3SBH)SO_4\cdot H_2O}$	T (K)	299.4	265.4	222.0	194.2	152.8	107.6	96.7	78.0
$\theta = -3.5$ K	χ_M (cgsu)	11648	12942	15237	17284	21630	30003	33254	41226
	μ_{eff} (μ_B)	5.28	5.24	5.20	5.18	5.14	5.08	5.07	5.07
$\mathrm{Fe(5\text{-}NO_2SBH)SO_4\cdot H_2O}$	T (K)	297.2	257.8	216.4	198.0	153.2	107.8	97.6	78.0
$\theta = -3.0$ K	χ_M (cgsu)	11646	13222	15631	16822	21573	30065	33077	41064
	μ_{eff} (μ_B)	5.26	5.22	5.20	5.16	5.14	5.09	5.08	5.06
$\mathrm{Co(H{-}SBH)Cl\cdot 2H_2O}$	T (K)	300.0	258.4	216.6	192.0	153.6	110.4	98.0	78.0
$\theta = -3.0$ K	χ_M (cgsu)	8900	10066	11283	12729	15767	20951	22948	28023
	μ_{eff} (μ_B)	4.62	4.56	4.42	4.42	4.40	4.30	4.24	4.18
$\mathrm{Co(3\text{-}NO_2SBH)Cl\cdot 2H_2O}$	T (K)	300.0	259.6	217.6	192.4	154.6	109.6	97.8	78.0
$\theta = -4.0$ K	χ_M (cgsu)	8632	9976	11231	12588	15241	21104	23213	28833
	μ_{eff} (μ_B)	4.55	4.55	4.42	4.40	4.34	4.30	4.26	4.24
$\mathrm{Co(3\text{-}CH_3OSBH)Cl\cdot 2H_2O}$	T (K)	298.8	261.0	216.0	194.2	152.0	108.6	97.2	78.0
$\theta = -3.0$ K	χ_M (cgsu)	8328	9279	10908	11910	14935	20514	22703	28023
	μ_{eff} (μ_B)	4.46	4.40	4.34	4.30	4.26	4.22	4.20	4.18
$\mathrm{Co(5\text{-}ClSBH)Cl\cdot 2H_2O}$	T (K)	297.6	256.2	218.0	196.0	155.5	110.0	96.8	78.0
$\theta = -4.0$ K	χ_M (cgsu)	8894	10064	11620	12696	16002	21028	23453	28291
	μ_{eff} (μ_B)	4.60	4.54	4.50	4.46	4.38	4.30	4.26	4.20
$\mathrm{Co(5\text{-}BrSBH)Cl\cdot 2H_2O}$	T (K)	298.2	262.0	217.0	190.0	156.2	112.2	98.2	78.0
$\theta = -3.5$ K	χ_M (cgsu)	8924	9928	11364	12631	14946	20044	22472	28023
	μ_{eff} (μ_B)	4.62	4.56	4.44	4.38	4.32	4.24	4.20	4.18
$\mathrm{Co(5\text{-}NO_2SBH)Cl\cdot 2H_2O}$	T (K)	298.6	259.4	218.4	198.2	158.0	107.0	97.6	78.0
$\theta = -5.0$ K	χ_M (cgsu)	8788	9852	11393	12108	14639	21217	22610	28291
	μ_{eff} (μ_B)	4.58	4.52	4.46	4.38	4.30	4.26	4.20	4.20
$\mathrm{Cu(H{-}SBH)Cl\cdot H_2O}$	T (K)	300.0	261.0	211.0	197.0	156.0	108.0	97.2	78.0
$\theta = -5.0$ K	χ_M (cgsu)	1473	1622	1920	2012	2512	3547	3807	4526
	μ_{eff} (μ_B)	1.88	1.84	1.80	1.78	1.77	1.75	1.72	1.68
$\mathrm{Cu(3\text{-}NO_2SBH)Cl\cdot H_2O}$	T (K)	299.2	259.0	211.8	194.2	154.5	107.6	96.0	78.0
$\theta = -6.0$ K	χ_M (cgsu)	1446	1564	1871	1995	2395	3281	3634	4526
	μ_{eff} (μ_B)	1.86	1.80	1.78	1.76	1.72	1.68	1.67	1.66
$\mathrm{Cu(3\text{-}CH_3OSBH)Cl\cdot H_2O}$	T (K)	300.0	263.0	208.9	192.7	153.0	109.0	98.0	78.0
$\theta = -6.5$ K	χ_M (cgsu)	1473	1610	1897	2010	2475	3239	3517	4366
	μ_{eff} (μ_B)	1.88	1.84	1.78	1.76	1.74	1.68	1.66	1.65
$\mathrm{Cu(5\text{-}ClSBH)Cl\cdot H_2O}$	T (K)	300.0	260.0	209.8	197.0	154.0	108.0	97.0	78.0
$\theta = -5.5$ K	χ_M (cgsu)	1473	1597	1889	1967	2459	3347	3640	4419
	μ_{eff} (μ_B)	1.88	1.82	1.78	1.76	1.74	1.70	1.68	1.66
$\mathrm{Cu(5\text{-}BrSBH)Cl\cdot H_2O}$	T (K)	299.0	262.2	208.9	196.7	152.8	107.8	98.2	78.0
$\theta = -5.0$ K	χ_M (cgsu)	1478	1615	1983	2015	2564	3553	3595	4419
	μ_{eff} (μ_B)	1.88	1.84	1.82	1.78	1.77	1.75	1.68	1.66
$\mathrm{Cu(5\text{-}CH_3SBH)Cl\cdot H_2O}$	T (K)	297.0	258.0	209.0	197.8	155.6	108.2	97.2	78.0
$\theta = -4.5$ K	χ_M (cgsu)	1488	1677	1982	2003	2490	3500	3719	4526
	μ_{eff} (μ_B)	1.88	1.86	1.82	1.78	1.76	1.74	1.70	1.68
$\mathrm{Cu(5\text{-}NO_2SBH)Cl\cdot H_2O}$	T (K)	299.8	259.8	208.7	196.6	153.7	109.2	98.7	78.0
$\theta = -5.0$ K	χ_M (cgsu)	1443	1595	1899	1971	2464	3389	3577	4419
	μ_{eff} (μ_B)	1.86	1.82	1.78	1.76	1.74	1.72	1.68	1.66

[13], as partly confirmed by the upward displacement of the amide **II** ($\Delta\nu$(CH) + δ(NH) $\simeq$ 30 cm^{-1}) and amide **IV** ($\Delta\delta$(C=O) $\simeq$ 20 cm^{-1}) and the downward displacement of amide **I** ($\Delta\nu$(C=O) $\simeq$ 40 cm^{-1}) and amide **III** ($\Delta\delta$(NH) $\simeq$ 15 cm^{-1}) bands, except in the spectra of the Fe(III), Co(II), Ni(II) and Zn(II) complexes. These complexes do not show any characteristic bands of amino and amide groups, showing that the ligands are coordinated in the enolic form [14].

The coordination of the azomethine nitrogen atom to the metal ions is indicated by displacement of bands mainly assigned to the ν(C=N) and ν(N–N) stretching vibrations. The spectra of the complexes show a downward displacement of ν(C=N) from *ca.* 1630 cm^{-1} for XSBH to *ca.* 1595 cm^{-1}, and ν(N–N) from *ca.* 980 cm^{-1} to *ca.* 965 cm^{-1}. These changes indicate coordination of the azomethine nitrogen atom to the metal ion [15].

In the far-infrared region the Fe(III), Co(II), Ni(II) and Zn(II) complexes show bands at *ca.* 445, *ca.* 420, *ca.* 395 and *ca.* 340 cm^{-1} which are assigned to ν(M–O) phenolic, ν(M–N), ν(M–O)·H_2O and ν(M–O) enolic vibrations, respectively. The Fe(III), Co(II) and Ni(II) complexes also show a band at *ca.* 410 cm^{-1} for the ν(M–Cl) stretching vibration [16]. The Mn(II), Cu(II) and Pt(II) complexes show bands at *ca.* 440, *ca.* 430, *ca.* 395 and *ca.* 345 cm^{-1}, which are assigned to ν(M–O) phenolic, ν(M–N), ν(M–O)·H_2O and ν(M–O) ketonic, respectively [16]. The monodentate coordination of the sulphate group is indicated by the appearance of a ν(S–O) band at *ca.* 990 cm^{-1} and ν(Fe–OSO_3) at *ca.* 250 cm^{-1} in Fe(II) complexes [16, 17].

The magnetic susceptibility data for the metal complexes are reported in Table II. The Zn(II) and Pt(II) complexes are diamagnetic. The magnetic moments of Mn(II) complexes are typical of a high-spin type and do not show any significant change over the temperature range studied [18].

The Fe(III) complexes have magnetic moments in the range 5.24–5.17 μ_B, showing the presence of high-spin Fe(III) ions, at room temperature and also at 78 K. Plots of magnetic data for Fe(H–SBH)Cl complex are illustrated in Fig. 1. This behaviour is a reflection of an intermolecular antiferromagnetic exchange interaction between the two $S = 5/2$ ions in the dimeric Fe(III) complex [19]. Such an exchange interaction between two $S = 5/2$ ions can be largely accounted for by an isotropic exchange spin Hamiltonian of the form $\mathcal{H} = -2J\hat{S}_i\cdot\hat{S}_2$, where S_i is the spin operator on each of the two metal centres and J is the exchange parameter, which is a gauge of the magnitude of the interaction. An exchange coupled $S_i = S_2 = 5/2$ complex has electronic states with a total spin of $S' = 5, 4, 3, 2, 1$ and 0. It is characteristic of such an interacting ferric dimer that, even for a weak interaction, the variation in Boltzmann distribution over S' states as a function of temperature is gradual and has an effect even at high temperature. Thus, even weak antiferromagnetic exchange interactions can influence the μ_{eff} values at *ca.* 298 K and this could partially explain why the observed values are below the spin-only value of 5.9 μ_B.

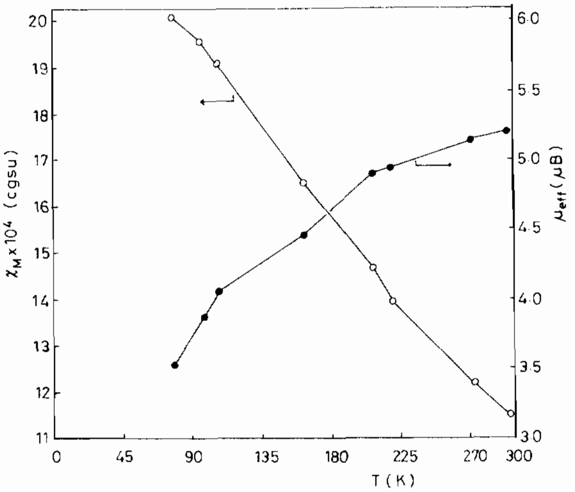

Fig. 1. Magnetic susceptibility (χ_M) and effective magnetic moment (μ_{eff}, μ_B) *vs.* temperature (K) for Fe(HSBH)Cl.

The variable-temperature magnetic susceptibility data for Fe(XSBH)Cl were fitted to the theoretical equation [18] to give $J = ca.$ −8.0 cm^{-1} and $g = 2.00$. It can be seen that the fits are reasonable, which verifies the suggestion that there is an antiferromagnetic exchange interaction present in dimeric complexes. The magnitude of the latter interaction is a reflection of the details of the electronic structure of bridged species and does not depend simply on the Fe–Fe distance [20].

The Fe(II) complexes show magnetic moments ranging from 5.26–5.29 μ_B at room temperature, to 5.05–5.07 μ_B at liquid N_2 temperature, which are consistent with those reported for five-coordinate Fe(II) complexes [21] and lower than that of six-coordinate complexes ($\mu_{eff} = 5.5$ μ_B) [22]. The presence of axial ligands in the five-coordination sphere would generate a large splitting of the $^5T_2$ state (of O_h origin), thereby reducing the orbital contribution to μ_{eff}.

The magnetic moment of dimeric Co(II) complexes are partially affected by what appear to be very weak antiferromagnetic interactions [23, 24], while the dimeric Ni(II) complexes exhibit anomalous magnetic moments (*ca.* 1.10 μ_B), which lie in between the values expected for either high- or low-spin Ni(II) complexes, regardless of the coordination geometry about the metal. Several mechanisms may be given for μ_{eff} values of these complexes with O*–N*–O* containing ligands [5]. The Ni(II) complexes are known to exist as high- or low-spin complexes depending upon the π-bonding character of the ligand donor atoms [25]. A spin-state isomerism between singlet and triplet states for a distorted five-coordinate complex is predicted for Ni(II) complexes, based on the interpretation of their visible spectra (*vide infra*).

The Cu(II) complexes usually show magnetic moment values corresponding to spin-only for one electron which are in the range normally observed for these complexes having an orbitally non-degenerate ground state. The magnitude and slight temperature dependence of the magnetic moments rules out the presence of Cu–Cu interaction in the complexes [18, 26].

TABLE III. Mössbauer Spectral Data of Iron(II) and Iron(III) Complexes

Compound	Temperature (K)	ΔE_Q (mm/s)	δ^a (mm/s)	$\Gamma_1{}^b$ (mm/s)	$\Gamma_2{}^b$ (mm/s)
Fe(H–SBH)$SO_4 \cdot H_2O$	4.2	4.02	1.22	0.28	0.32
	78	3.96	1.14	0.26	0.30
	298	3.82	1.01	0.23	0.28
Fe(3-CH_3OSBH)$SO_4 \cdot H_2O$	4.2	4.01	1.18	0.30	0.36
	78	3.98	1.16	0.28	0.33
	298	3.89	1.02	0.25	0.31
Fe(3-NO_2SBH)$SO_4 \cdot H_2O$	4.2	4.03	1.16	0.32	0.36
	78	3.89	1.13	0.30	0.33
	298	3.87	1.01	0.29	0.31
Fe(5-ClSBH)$SO_4 \cdot H_2O$	4.2	4.01	1.12	0.36	0.37
	78	3.98	1.09	0.34	0.34
	298	3.88	1.04	0.30	0.32
Fe(5-BrSBH)$SO_4 \cdot H_2O$	4.2	4.02	1.14	0.30	0.34
	78	3.99	1.11	0.26	0.29
	298	3.89	1.02	0.22	0.27
Fe(5-CH_3SBH)$SO_4 \cdot H_2O$	4.2	4.04	1.12	0.34	0.36
	78	4.01	1.09	0.31	0.34
	298	3.90	1.02	0.28	0.32
Fe(5-NO_2SBH)$SO_4 \cdot H_2O$	4.2	4.00	1.16	0.31	0.34
	78	3.96	1.12	0.28	0.27
	298	3.88	1.04	0.20	0.23
Fe(H–SBH)Cl	4.2	1.46	0.56	0.22	0.24
	78	1.42	0.50	0.19	0.20
	298	1.39	0.44	0.17	0.18
Fe(3-CH_3OSBH)Cl	4.2	0.56	0.48	0.34	0.32
	78	0.53	0.42	0.26	0.25
	298	0.50	0.36	0.22	0.20
Fe(3-NO_2SBH)Cl	4.2	0.58	0.46	0.36	0.33
	78	0.55	0.40	0.32	0.31
	298	0.52	0.34	0.29	0.26
Fe(5-ClSBH)Cl	4.2	0.58	0.42	0.29	0.34
	78	0.54	0.40	0.25	0.30
	298	0.52	0.32	0.22	0.26
Fe(5-BrSBH)Cl	4.2	0.54	0.42	0.30	0.33
	78	0.50	0.39	0.27	0.31
	298	0.48	0.34	0.24	0.26
Fe(5-CH_3SBH)Cl	4.2	0.54	0.44	0.30	0.31
	78	0.51	0.38	0.28	0.28
	298	0.50	0.32	0.26	0.27
Fe(5-NO_2SBH)Cl	4.2	0.52	0.40	0.29	0.30
	78	0.90	0.38	0.26	0.28
	298	0.49	0.34	0.24	0.25

[a] Relative to natural iron foil. [b] Full width at half-maximum for low velocity line Γ_1 and high-velocity line Γ_2.

The ^{57}Fe Mössbauer spectra of iron(II) and iron(III) complexes have been measured at 278, 78 and 4.2 K (Table III). The chemical isomer shift, δ, relative to natural iron foil, which is sensitive to both the oxidation state and the spin state of the iron, is characteristic of distorted high-spin, five-coordinate Fe(II) complexes [27]. The fact that the δ values increase with decreasing temperature can be attributed to a second-order Döppler shift arising from a lattice effect.

The quadrupole splitting parameter, ΔE_Q, is sufficiently large and is characteristic of five-coordinate Fe(II) complexes. The large values of ΔE_Q for these complexes are assumed to be caused by a large contribution of like sign from both the non-spherical electron distribution and the ligand-field dissymmetry [28]. The contribution to ΔE_Q from the dissymmetry of the d-electron population will depend upon the nature of the ground state. The magnitude of the contribution to ΔE_Q from a 3d electron in either d_{xy} or d_{xz}, d_{yz} are equal, but the electric field gradients associated with these two states are of opposite signs. The results of the magnetically perturbed Mössbauer spectrum of a five-coordinate high-spin Fe(II) complex imply [29] that the ground state is d_{xy} ($^5B_2$), contrary to the ordering of the one-electron d orbitals expected from crystal-field theory for both the square-pyramidal or trigonal-bipyramidal geometries [29]. Thus, on the basis of this result, it is assumed that the ground state in these complexes is $^5B_2$.

The observed values of δ and ΔE_Q are indicative of a dimeric, high-spin, five-coordinate structure for Fe(XSBH)Cl complexes [27]. The Mössbauer spectra of Fe(HSBH)Cl at various temperatures are illustrated in Fig. 2. Essentially identical spectra to the Fe(HSBH)Cl complex were obtained for the remaining Fe(III) complexes. The large quadrupole splitting in Fe(III) complexes is most probably due to the large electric field gradient at the nucleus resulting from the open coordination site. The observed asymmetry in the intensity of the two quadrupole split lines, which is apparent in Fig. 2 of this Fe(HSBH)Cl complex, is characteristic of complexes of this type [20, 27, 30]. Although this asymmetry could result from partial orientation of sample crystallites in the sample container, as observed for $Fe_2(CO)_9$ [31], this seems unlikely because the asymmetry tends to decrease with decreasing temperature. It appears that the asymmetry in the two quadrupole split lines and its temperature dependence are most probably due to intermolecular spin spin relaxation [32].

The polycrystalline ESR spectra of Cu(II) complexes are of axial type with a primarily $d_{x^2-y^2}$ ground state in a square-planar structure [26, 33]. ESR spectral data of all Cu(II) complexes are presented in Table IV.

The free ligands exhibit absorption bands at *ca.* 41 670, *ca.* 38 460 and *ca.* 31 750 cm^{-1} in the UV region, which are assigned to $n \rightarrow \sigma^*$, $\pi \rightarrow \pi^*$ and $n \rightarrow \pi^*$ transitions, respectively [5]. The high absorption by these ligands masks any splitting of bands and only slight wavelength and intensity variations are significant in the metal complexes. The spectra of the complexes are dominated by the ligand absorption bands.

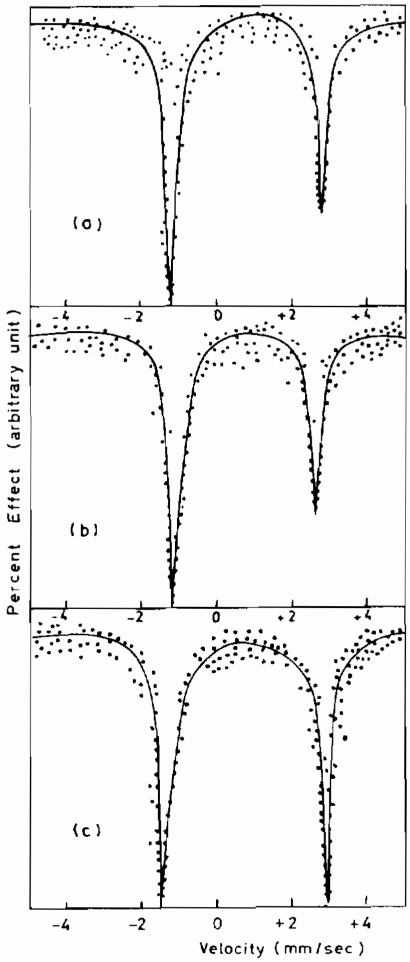

Fig. 2. Mössbauer spectrum of Fe(HSBH)Cl at: (a) 298 K, (b) 78 K, (c) 4.2 K.

Very intense transitions are observed in the visible spectra of the Mn(II) complexes at *ca.* 18 000 and *ca.* 25 000 cm^{-1}, which are assigned [34] as $\pi \rightarrow eg^*$ and $eg \rightarrow \pi^*$ transitions, respectively.

The Fe(II) complexes in the visible–near IR region show two broad ligand-field absorption bands at *ca.* 5400 and *ca.* 9000 cm^{-1}, which are assigned to the $^5A_1$ and $^5B_1$ states derived from the splitting of the ^5E spectroscopic term in the tetragonal ligand field [21]. The splitting (*ca.* 4000 cm^{-1}) of the ^5E excited state indicates a highly distorted ligand field in these complexes. In Fe(II) complexes Fe($t_{2g} \rightarrow \pi^*$) XSBH transition is also exhibited at *ca.* 21 000 cm^{-1} [34].

TABLE IV. ESR Data of Copper(II) Complexes

Compound	$g_\perp$	$g_\parallel$	G^a
$Cu(H{-}SBH)Cl\cdot H_2O$	2.040(g_1) 2.146(g_2)	2.301(g_3)	2.1623
$Cu(3\text{-}NO_2SBH)Cl\cdot H_2O$	2.064	2.270	2.1332
$Cu(3\text{-}CH_3OSBH)Cl\cdot H_2O$	2.066	2.273	2.1350
$Cu(5\text{-}ClSBH)Cl\cdot H_2O$	2.065	2.271	2.1336
$Cu(5\text{-}BrSBH)Cl\cdot H_2O$	2.070	2.274	2.1380
$Cu(5\text{-}CH_3SBH)Cl\cdot H_2O$	2.068	2.273	2.1363
$Cu(5\text{-}NO_2SBH)Cl\cdot H_2O$	2.072	2.275	2.1360

$^a G = 1/3(2g_\perp + g_\parallel)$ or $1/3(g_1 + g_2 + g_3)$.

The Fe(XSBH)Cl complexes exhibit a single band at 11 000 cm^{-1}, which can be assigned to a ligand-field transition. This transition is a common feature of five-coordinate Fe(III) complexes [8, 20, 35].

The spectra of the Co(II) complexes are very similar to the spectra of dihalo-bis(2-dimethylaminoethyl)methylamine Co(II) complexes for which C_{2v} symmetry has been confirmed [36, 37]. Thus the well-defined spectral bands centred at *ca.* 5000, *ca.* 10 000 and *ca.* 16 600 cm^{-1} are assigned to the spin-allowed transitions $^4A_2'(F) \rightarrow {}^4E''(F)$, $^4A_2'(F) \rightarrow {}^4E'(F)$ and $^4A_2'(F) \rightarrow {}^4A_2'(P)$, respectively. The spectral band corresponding to the transition $^4A_2'(F) \rightarrow {}^4E''(P)$, which is observed at 20 000 cm^{-1} in dihalo-bis(2-dimethylaminoethyl)methylamine Co(II) complexes, is obscured by strong charge-transfer bands in the spectra of the present complexes.

The spectra of the Ni(II) complexes exhibit two bands at *ca.* 16 260 and *ca.* 22 750 cm^{-1}. The lower energy band is similar to that for low-spin five-coordinate Ni(II) complexes [25] and is assigned to the transition $d_{xy}, d_{x^2-y^2} \rightarrow d_{z^2}$ in a trigonal-bipyramidal environment. The higher energy band is assigned to the $d_{xz}, d_{yz} \rightarrow d_{z^2}$ transition.

The Cu(II) complexes exhibit a characteristic band at *ca.* 14 500 cm^{-1}, which is assigned to $^5B_{1g} \rightarrow {}^2A_{1g}$, $^2B_{2g}$, ^2E_g transitions in a square-planar geometry [38].

The spectra of the $Pt(XSBH)Cl\cdot H_2O$ complexes display two spectral bands at *ca.* 17 860 and *ca.* 20 500 cm^{-1}, which are assigned to a metal-to-ligand (Pt(II) → π^* XSBH) charge-transfer transition [15].

Antitumor Activity

The antitumor activity of all compounds was tested at the National Cancer Institute, Bethesda, Md. by the standard screening procedure (cf. Instruction 14) in the P388 lymphocytic leukaemia test system [39]. The tumor inoculum of 10^6 ascites cells was injected intraperitoneally (ip) on day zero in CD_2F_1 (CDF_1) mice (female). The compounds were suspended in saline with Tween 80 and administered daily ip in accordance with the treatment schedule indicated in Table V. Six mice were used per test compound and the compound was considered to be active when the *T/C%* (test/control) value was more than 125.

All the compounds show no significant activity and are toxic at the doses used. This is a surprising finding as metal chelates of aroylhydrazones, particularly Cu(II) complexes, have been shown to be potent inhibitors of DNA synthesis and cell growth in a variety of human and rodent cell lines grown in culture [40]. The screening data are reported in Table V.

TABLE V. Antitumor Activity of the Metal Complexes

Compound	Dose (mg/kg)	Weight difference (*T* – *C*)	*T/C* (%)
H–SBH	400	–2.5	105
	200	–2.4	95
	100	–2.0	90
	50	–1.1	110
	25	–1.0	108
$3\text{-}NO_2SBH$	400	–2.0	96
	200	–2.2	92
	100	–1.2	90
	50	0.8	90
$3\text{-}CH_3OSBH$	400	–0.8	100
	200	–0.5	90
	100	–0.3	90
	50	1.0	90
5-ClSBH	400	–2.7	90
	200	–2.0	100
	100	–1.2	95
5-BrSBH	400	–2.5	95
	200	–2.0	90
	100	–1.8	95
	50	0.8	95
	25	0.3	100

(continued)

TABLE V. *(continued)*

Compound	Dose (mg/kg)	Weight difference (*T* – *C*)	*T*/*C* (%)
5-CH$_3$SBH	400	2.0	100
	200	1.7	95
	100	1.0	95
5-NO$_2$SBH	240	1.6	95
	120	1.5	95
	60	0.8	90
	30	0.5	90
Mn(H–SBH)$_2$	240		toxic
	120		toxic
	60	-1.5	85
	30	-1.0	80
Mn(3-NO$_2$SBH)$_2$	400	-2.0	95
	200	-1.6	90
	100	-1.0	90
	50	-0.5	88
Mn(3-CH$_3$OSBH)$_2$	400		toxic
	200		toxic
	100		toxic
	50	0.3	80
Mn(5-ClSBH)$_2$	240		toxic
	120		toxic
	60	-2.3	80
	30	-1.0	85
Mn(5-BrSBH)$_2$	240		toxic
	120	-1.0	85
	60	0.8	85
	30	0.2	80
Mn(5-CH$_3$SBH)$_2$	400	-2.0	100
	200	-1.5	80
	100	-1.0	80
	50	-0.5	85
Mn(5-NO$_2$SBH)$_2$	400		toxic
	200		toxic
	100		toxic
Fe(H–SBH)Cl	400	-2.0	80
	200	-1.0	85
	100	-0.5	90
Fe(3-NO$_2$SBH)Cl	240		toxic
	120		toxic
	60		toxic
Fe(3-CH$_3$OSBH)Cl	240		toxic
	120		toxic
	60	-1.0	80
Fe(5-ClSBH)Cl	400		toxic
	200	-2.3	89
	100	-2.0	80
	50	-1.8	80
Fe(5-BrSBH)Cl	400	-1.9	100
	200	-1.6	90
	100	-1.0	90

(continued)

TABLE V. *(continued)*

Compound	Dose (mg/kg)	Weight difference (*T* – *C*)	*T*/*C* (%)
Fe(5-CH$_3$SBH)Cl	240		toxic
	120		toxic
	60		toxic
Fe(5-NO$_2$SBH)Cl	240		toxic
	120		toxic
	60	-2.0	85
Fe(H–SBH)SO$_4$·H$_2$O	240		toxic
	120		toxic
	60	-1.0	80
Fe(3-NO$_2$SBH)SO$_4$·H$_2$O	400	-2.6	100
	200	-2.0	95
	100	-1.8	90
	50	-1.5	105
Fe(3-CH$_3$OSBH)SO$_4$·H$_2$O	400		toxic
	200		toxic
	100	-1.2	80
Fe(5-ClSBH)SO$_4$·H$_2$O	400	-1.6	90
	200	1.0	85
	100	0.8	80
Fe(5-BrSBH)SO$_4$·H$_2$O	240	1.3	80
	120	1.0	80
	60	0.2	95
Fe(5-CH$_3$SBH)SO$_4$·H$_2$O	240	-2.2	85
	120	1.2	90
	60	-1.0	100
Fe(5-NO$_2$SBH)SO$_4$·H$_2$O	240		toxic
	120		toxic
	60	-1.5	85
Co(H–SBH)Cl·2H$_2$O	400		toxic
	200		toxic
	100		toxic
Co(3-NO$_2$SBH)Cl·2H$_2$O	240	-2.1	85
	120	-1.9	85
	60	-1.6	98
Co(3-CH$_3$OSBH)Cl·2H$_2$O	240		toxic
	120		toxic
	60	-2.0	85
Co(5-ClSBH)Cl·2H$_2$O	400		toxic
	200	-2.5	90
	100	-2.0	80
	50	0.8	100
Co(5-BrSBH)Cl·2H$_2$O	400		toxic
	200	-1.6	100
	100	-0.8	102
Co(5-CH$_3$SBH)Cl·2H$_2$O	400		toxic
	200		toxic
	100		toxic
Co(5-NO$_2$SBH)Cl·2H$_2$O	240		toxic
	120		toxic
	60		toxic
	30	-1.1	90

(continued)

TABLE V. *(continued)*

Compound	Dose (mg/kg)	Weight difference ($T - C$)	T/C (%)
$\mathrm{Ni(H-SBH)Cl\cdot 2H_2O}$	400		toxic
	200	−1.8	85
	100	−0.5	80
$\mathrm{Ni(3\text{-}NO_2SBH)Cl\cdot 2H_2O}$	240		toxic
	120		toxic
	60		toxic
	30		toxic
$\mathrm{Ni(3\text{-}CH_3OSBH)Cl\cdot 2H_2O}$	240		toxic
	120		toxic
	60		toxic
	30	−2.4	80
$\mathrm{Ni(5\text{-}ClSBH)Cl\cdot 2H_2O}$	240	−2.8	100
	120	−2.0	90
	60	−1.6	90
$\mathrm{Ni(5\text{-}BrSBH)Cl\cdot 2H_2O}$	240	−2.0	100
	120	−1.4	105
	60	−1.0	90
$\mathrm{Ni(5\text{-}CH_3SBH)Cl\cdot 2H_2O}$	400	−2.4	100
	200	−2.0	95
	100	−1.0	80
$\mathrm{Ni(5\text{-}NO_2SBH)Cl\cdot 2H_2O}$	400		toxic
	200		toxic
	100	−2.0	95
	50	−1.0	100
	25	−0.8	90
$\mathrm{Cu(H-SBH)Cl\cdot H_2O}$	400		toxic
	200		toxic
	100	−0.3	80
$\mathrm{Cu(3\text{-}NO_2SBH)Cl\cdot H_2O}$	240	−2.0	100
	120	−1.7	90
	60	−1.0	95
$\mathrm{Cu(3\text{-}CH_3OSBH)Cl\cdot H_2O}$	240		toxic
	120		toxic
	60		toxic
$\mathrm{Cu(5\text{-}ClSBH)Cl\cdot H_2O}$	240	−2.4	105
	120	−2.0	100
	60	−1.0	100
	30	−0.5	90
$\mathrm{Cu(5\text{-}BrSBH)Cl\cdot H_2O}$	240		toxic
	120	−1.8	95
	60	−1.0	80
$\mathrm{Cu(5\text{-}CH_3SBH)Cl\cdot H_2O}$	400		toxic
	200	−1.8	100
	100	−1.0	80
$\mathrm{Cu(5\text{-}NO_2SBH)Cl\cdot H_2O}$	240		toxic
	120		toxic
	60	−0.3	85
$\mathrm{Zn(H-SBH)}$	240	−2.2	95
	120	−1.8	90
	60	−1.0	80
$\mathrm{Zn(3\text{-}NO_2SBH)}$	400		toxic
	200		toxic
	100		toxic
$\mathrm{Zn(3\text{-}CH_3OSBH)}$	400	−1.8	80
	200	−1.2	85
	100	−0.8	80
$\mathrm{Zn(5\text{-}ClSBH)}$	400		toxic
	200		toxic
	100		toxic
$\mathrm{Zn(5\text{-}BrSBH)}$	400	−2.4	80
	200	−2.0	85
	100	−1.6	80
$\mathrm{Zn(5\text{-}CH_3SBH)}$	400		toxic
	200		toxic
	100	−2.0	80
$\mathrm{Zn(5\text{-}NO_2SBH)}$	240	−2.2	100
	120	−2.0	90
	60	−1.0	80
$\mathrm{Pt(H-SBH)Cl\cdot H_2O}$	400	−1.9	80
	200	−1.5	85
	100	−1.0	90
	50	−0.4	85
$\mathrm{Pt(3\text{-}NO_2SBH)Cl\cdot H_2O}$	240		toxic
	120		toxic
	60		toxic
	30	−0.8	85
$\mathrm{Pt(3\text{-}CH_3OSBH)Cl\cdot H_2O}$	240		toxic
	120	−1.8	95
	60	−1.0	85
$\mathrm{Pt(5\text{-}ClSBH)Cl\cdot H_2O}$	400	−2.0	90
	200	−1.0	90
	100	−0.5	80
$\mathrm{Pt(5\text{-}BrSBH)Cl\cdot H_2O}$	400		toxic
	200		toxic
	100	−2.3	100
	50	−0.8	80
$\mathrm{Pt(5\text{-}CH_3SBH)Cl\cdot H_2O}$	240		toxic
	120		toxic
	60		toxic
$\mathrm{Pt(5\text{-}NO_2SBH)Cl\cdot H_2O}$	400	−2.7	90
	200	−2.3	100
	100	−2.0	108
	50	−0.8	90

Acknowledgements

We are grateful to Dr R. Bembi, Roorkee University, Roorkee, for magnetic data and Mössbauer spectral data, and the authorities of RSIC, I.I.T., Madras for UV–Vis and ESR data.

References

1 H. Ohta, *Chem. Soc. (Jpn.), 31,* 1056 (1958); *33,* 2 (1960).
2 A. Jacobs, *Br. J. Haematol., 43,* 1 (1979).
3 C. Hershco, S. Avramovici-Grisaru, G. Link, L. Gelfand and S. Sarel, *J. Lab. Clin. Med., 98,* 99 (1981).
4 L. Pickart, W. H. Goodwin, T. B. Murphy and D. K. Johnson, *J. Cell. Biochem. Suppl, 6,* L482 (1982).
5 M. Mohan, A. Kumar, M. Kumar and N. K. Jha, *Inorg. Chim. Acta, 136,* 65 (1987) and refs. therein.
6 M. Mohan, N. S. Gupta, L. Chandra and N. K. Jha, *J. Inorg. Biochem., 31,* 7 (1987).
7 W. J. Geary, *Coord. Chem. Rev., 7,* 81 (1971).
8 M. Mohan and M. Kumar, *Polyhedron, 4,* 1929 (1985).
9 R. J. Butcher, J. Jasinki, G. M. Mockler and E. Sinn, *J. Chem. Soc., Dalton Trans.,* 1099 (1976).
10 J. O. Miners, E. Sinn, R. B. Coles, and C. M. Harris, *J. Chem. Soc., Dalton Trans.,* 1149 (1976).
11 D. J. Hewkin and W. P. Griffith, *J. Chem. Soc. A,* 472 (1966).
12 W. P. Griffith, *J. Chem. Soc. A,* 211 (1969).
13 M. Nonoyama, S. Tomita and K. Yamasaki, *Inorg. Chim. Acta, 12,* 33 (1975).
14 C. N. R. Rao, 'Chemical Applications of Infrared Spectroscopy', Academic Press, New York/London, 1962.
15 M. Mohan, P. Sharma, M. Kumar and N. K. Jha, *Inorg. Chim. Acta, 125,* 9 (1986).
16 J. R. Ferraro, 'Low-Frequency Vibrations of Inorganic and Coordination Compounds', Plenum Press, New York, 1971.
17 T. B. Murphy, N. J. Bose, V. Schomaker and A. Aruffo, *Inorg. Chim. Acta, 108,* 183 (1985).
18 A. Earnshaw, 'Magnetochemistry', Academic Press, New York, 1968.
19 J. Lewis, F. E. Mabbs and A. Richards, *J. Chem. Soc. A,* 1014 (1967).
20 W. M. Reiff, G. J. Long and W. A. Baker, Jr., *J. Am. Chem. Soc., 90,* 6347 (1968).
21 M. Mohan, S. G. Mittal, H. C. Khera and A. K. Sirivastava, *Gazz. Chim. Ital., 107,* 393 (1978).
22 G. J. Long and W. A. Baker, Jr., *J. Chem. Soc. A,* 2956 (1971).
23 L. Sacconi, M. Ciampolini and G. P. Speroni, *J. Am. Chem. Soc., 87,* 3102 (1965).
24 A. Earnshaw, P. C. Hewlett, E. A. King and L. F. Larkworthy, *J. Chem. Soc. A,* 241 (1968).
25 L. Sacconi, *Transition Met. Chem., 4,* 227 (1968) and refs. therein.
26 B. J. Hathaway in I. N. Bradly, R. D. Gillard and R. F. Hudson (eds.), 'Essays in Chemistry', Vol. 2, Academic Press, New York, 1971, p. 61.
27 N. N. Greenwood and T. C. Gibb, Mössbauer Spectroscopy', Chapman and Hall, London, 1971.
28 D. P. Riley, P. H. Merrell, J. A. Stone and D. H. Busch, *Inorg. Chem., 14,* 490 (1975).
29 W. M. Reiff, *Inorg. Chem., 13,* 239 (1974).
30 K. S. Murray, *Coord. Chem. Rev., 12,* 1 (1974).
31 T. C. Gibb, R. Greatrex and N. N. Greenwood, *J. Chem. Soc. A,* 890 (1968).
32 A. N. Buckley, I. R. Herbert, B. D. Rumbold, G. V. H. Wilson and K. S. Murray, *J. Phys. Chem. Solids, 31,* 1423 (1970).
33 B. J. Hathaway and D. E. Billing, *Coord. Chem. Rev., 5,* 143 (1970).
34 M. Mohan and B. D. Paramhans, *Indian J. Chem., 19A,* 759 (1980).
35 M. Blume, *Phys. Rev. Lett., 14,* 96 (1968).
36 C. Furlani, *Coord. Chem. Rev., 3,* 141 (1968).
37 M. Ciampolini, *Struct. Bonding (Berlin), 6,* 52 (1969) and refs. therein.
38 I. M. Procter, B. J. Hathaway and P. Nicholls, *J. Chem. Soc. A,* 1678 (1968).
39 R. I. Geran, N. H. Greenberg, M. M. Macobnald, A. M. Schumacher and B. J. Abbott, *Cancer Chemother. Rep., 3,* 9 (1972).
40 L. Pickart, W. H. Goodwin, W. Burgua, T. B. Murphy and D. K. Johnson, *Biochem. Pharmacol., 32,* 3868 (1983).